European Journal of Immunology

Immunomodulation and immune therapies

Basic

Research Article

Avidity optimization of a MAGE-A1-specific TCR with somatic hypermutation

David Bassan, Yosi Meir Gozlan, Adi Sharbi-Yunger, Esther Tzehoval, Erez Greenstein, Lidor Bitan, Nir Friedman and Lea Eisenbach

Department of Immunology, Weizmann Institute of Science, Rehovot, Israel

A T-cell receptor (TCR) with optimal avidity to a tumor antigen can be used to redirect T cells to eradicate cancer cells via adoptive cell transfer. Cancer testis antigens (CTAs) are attractive targets because they are expressed in the testis, which is immune-privileged, and in the tumor. However, CTAs are self-antigens and natural TCRs to CTAs have low affinity/avidity due to central tolerance. We previously described a method of directed evolution of TCR avidity using somatic hypermutation. In this study, we made several improvements to this method and enhanced the avidity of the hT27 TCR, which is specific for the cancer testis antigen HLA-A2-MAGE-A1$_{278-286}$. We identified eight point mutations with varying degrees of improved avidity. Human T cells transduced with TCRs containing these mutations displayed enhanced tetramer binding, IFN-γ and IL2 production, and cytotoxicity. Most of the mutations have retained specificity, except for one mutant with extremely high avidity. We demonstrate that somatic hypermutation is capable of optimizing avidity of clinically relevant TCRs for immunotherapy.

Keywords: affinity · HLA-A2 · MAGE-A1 · somatic hypermutation (SHM) · TCR

Additional supporting information may be found online in the Supporting Information section at the end of the article.

Introduction

T-cell receptors (TCRs) recognize specific peptides bound to the major histocompatibility complex (MHC). CD8+ cytotoxic T cells (CTLs) recognize peptides from degraded cellular proteins presented on MHC class I molecules, which are found on nearly all of the cells in the body [1]. T cells can distinguish between healthy cells and infected or cancerous cells based on the presented peptide-MHC (pMHC) complexes. A CTL that recognizes a target cell can kill the target cell, as well as secrete cytokines such as IFN-γ, TNF-α, and IL2. Several immunotherapies, such as adoptive T-cell transfer (ACT), rely on the capability of T cells to eliminate cancer cells. In ACT, tumor-reactive T cells are transferred into a patient, usually after lymphodepletion to remove cells competing for cytokines and regulatory cells. TCR gene therapy, or TCR gene transfer, is a type of ACT in which T cells from the peripheral blood are redirected to target tumor cells via expression of an anti-tumor TCR [2,3].

One key factor to the effectiveness of TCR gene therapy is TCR affinity/avidity. Affinity is the attraction of a single TCR to a pMHC, and avidity is the accumulated attraction of several interactions. TCR avidity depends on a number of parameters, such as TCR affinity, flexibility, stability, pairing, clustering, and co-receptors. TCR-pMHC avidity is a critical signal for activation, and there is a narrow window of optimal avidity. T-cell activity is ultimately determined by the balance of stimulatory and inhibitory signals. T-cell responsiveness, or functional avidity, increases with TCR affinity/avidity, but there is a plateau at the higher end (K_D = 1–5 μM) of the physiological range (K_D = 1–100 μM) [4,5]. TCRs with affinity well above the physiological range can either

Correspondence: Prof. Lea Eisenbach
e-mail: lea.eisenbach@weizmann.ac.il

lose specificity in CD8+ cells (where CD is cluster of differentiation) [6,7] or have reduced activity [4,5].

TCR affinity also plays a major role in positive and negative selection in the thymus. T cells with functional TCRs that interact with pMHC complexes pass positive selection. T cells with TCRs with high affinity to self-antigens presented in the thymus do not pass negative selection [8]. This process, known as central tolerance, prevents autoimmunity, but also presents a challenge for TCR gene therapy. Most shared tumor antigens are tumor-associated antigens (TAAs), which are self-antigens that are overexpressed or aberrantly expressed on cancer cells. Thus, natural TCRs specific for shared TAAs have low affinity and reactivity due to central tolerance [9].

Therefore, a number of methods have been developed to obtain TCRs with higher affinity/avidity capable of eradicating tumors. One in vivo approach is to vaccinate mice transgenic for a human MHC molecule with a human TAA that is not subject to central tolerance in mice [10]. A common in vitro approach is to perform random mutagenesis of a small region, followed by screening in phage [11], yeast [12], or T-cell display [13]. Another common approach is to isolate allo-restricted T cells from HLA-mismatched donors with high affinity to the target TAA on a nonself HLA allele. We previously described an in vitro approach for TCR avidity maturation using somatic hypermutation (SHM) [14]. In nature, SHM optimizes affinity of antibodies in B cells. The enzyme activation-induced cytidine deaminase (AID) initiates SHM by mutating cytidine (C) to uracil (U) [15]. AID has a hotspot-motif, WRCH (where W = A/T, R = A/G, C that is deaminated, and H = A/C/T), or its complement motif, DGYW [16]. Mutations can be caused if the U is unrepaired or repaired by error-prone DNA-repair mechanisms. For any of these approaches, cross-reactivity and recognition of low levels of antigen must be carefully examined, because the resulting TCRs were not subject to central tolerance to the human proteome on the target HLA allele.

Target selection, TCR specificity, and TCR avidity are crucial factors in the efficiency and safety of TCR gene therapy targeting a TAA. There can be severe toxicities if a TAA is expressed on a vital organ at sufficient levels for recognition by the transferred TCR. Cancer testis antigens (CTAs) are attractive targets because they are mostly or exclusively expressed on the tumor and the testis, an immune-privileged organ. TCR gene therapy targeting NY-ESO-1, a CTA, was both effective and safe [17,18]. However, if the CTA is expressed in other vital tissues or there is cross-reactivity to antigens expressed in healthy tissues, there can be severe, even fatal, toxicities [19,20].

Previously, we enhanced the avidity of the mouse Pmel-1 TCR using SHM in 293TREx cells [14]. We identified mutations that improved avidity and activity in vitro and in vivo. In this study, we sought to use SHM to enhance a clinically relevant human TCR. Additionally, we made a number of improvements to the SHM-based TCR avidity maturation system. The target we selected is the MAGE-A1$_{278\text{-}286}$ peptide bound to HLA-A*02:01, a common human MHC-I molecule in the HLA-A2 family. MAGE-A1 is a cancer testis antigen that is expressed in a variety of malignancies, including multiple myeloma, melanoma, lung, breast, colon, and ovarian cancer [21]. Importantly, it has been confirmed that this is a CTA that is indeed expressed exclusively in the testis and tumors [10]. This target has two known TCRs. One is a low-affinity variant isolated from the human CTL27 clone [22], "hT27" [10], and another is a high-affinity variant isolated from mice transgenic for both human TCRαβ and HLA-A2, "T1367" [10]. In this study, we desire to enhance the avidity of hT27 using an upgraded SHM system in a T-cell-derived cell line, BWZ.36 cells [23]. Following SHM-driven optimization, we can then compare our mutant hT27 TCRs to the known high-affinity T1367 TCR. We hope to demonstrate that SHM is an efficient and robust strategy to generate clinically relevant human TCRs with optimal avidity. Additionally, enhanced hT27 TCRs can be considered for use in TCR gene therapy.

Results

Construction of SHM-driven TCR avidity maturation system in BWZ.36-derived cells

We previously developed a TCR-avidity maturation system using SHM in 293TREx cells, and enhanced the mouse Pmel-1 TCR. For enhancing the hT27 TCR, we made a number of improvements to the SHM system. First, we used a T-cell line, BWZ.36-CD8α [23,24]. These cells do not express an endogenous TCR and express β-galactosidase upon TCR activation because they carry an NFAT-LacZ reporter gene. This allows for expression of a TCR of choice and detection of TCR activation by the color change of chlorophenolred-ß-D-galactopyranoside (CPRG) from yellow to red due to cleavage by β-galactosidase. Second, we used a more active variant of AID, AID mut 7.3 [25]. We transduced BWZ.36-CD8α cells with CD3 to compensate for low endogenous expression. We then stably expressed tetracycline repressor (TetR) and tetracycline-inducible AID mut 7.3 (Tet-AID 7.3) using electroporation and selection. We needed to also transduce the cells with TetR to ensure that AID expression was dox dependent (Supporting Information Fig. S1). The cells ready for SHM-driven TCR avidity maturation were designated "BWZ-8S" (Fig. 1A).

Optimization of DNA sequence in CDR3 loops for SHM

An additional improvement for SHM is to modify the DNA sequence of the TCR for AID-driven SHM and expression in primary T cells. For high expression in primary T cells, we used a codon-optimized DNA sequence. In nature the DNA sequence of antibodies, which undergo SHM in B cells, has been fine tuned for SHM in the complementary determining regions (CDRs) that interact with the antigen [26]. We developed an algorithm to mimic this process for the DNA sequence of TCRs in the CDR3 loops, which interacts with the peptide. We maximized AID hotspots, WRCH/DGYW, and minimized AID coldspots, SYC/GRS.

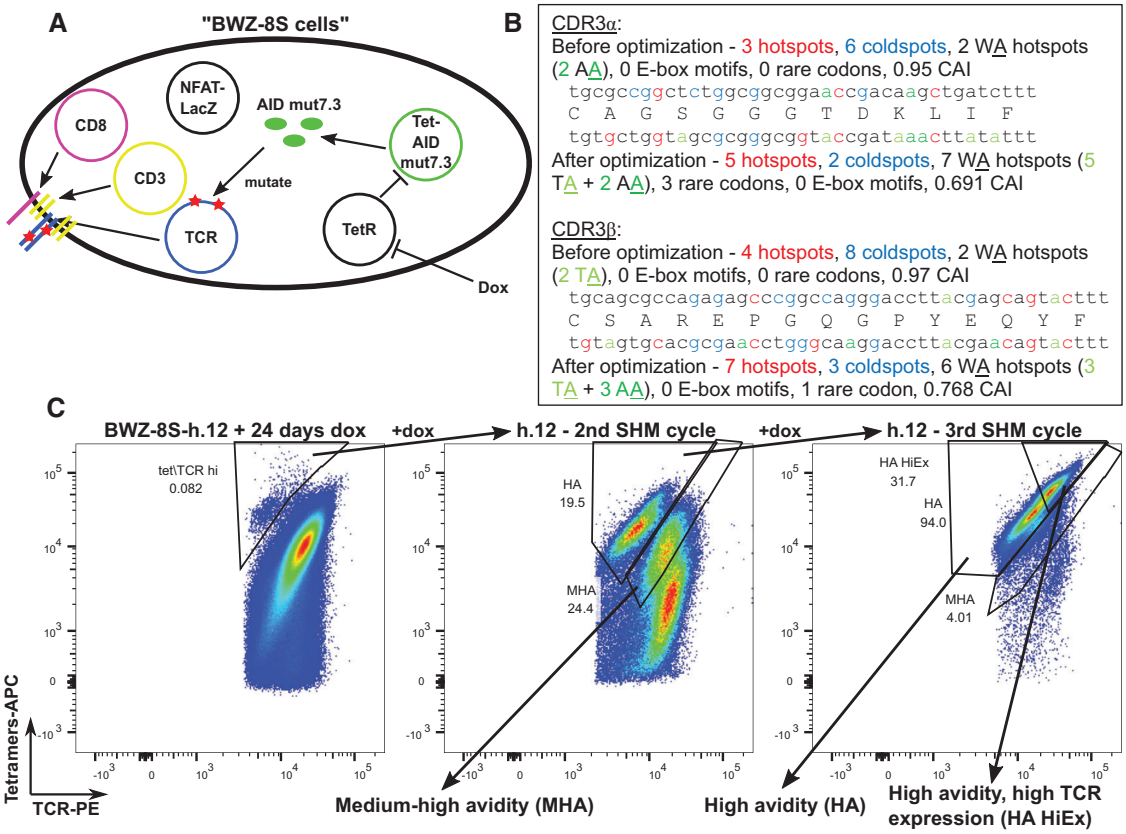

Figure 1. *SHM-based TCR avidity maturation system in BWZ.36-drived cells.* (A) Schematic representation of SHM system in "BWZ-8S" cells. Text surrounded by circles represents plasmids. TetR and Tet-AID (AID under regulation by TetR) plasmids allow for inducible expression of AID. The NFAT-LacZ reporter allows for using CPRG to detect TCR signaling, which activates the transcription factor NFAT. (B) DNA sequence for CDR3α (upper) and CDR3β (lower) of hT27 TCR before optimization above protein sequence and after optimization below protein sequence. Amino acid letter is at the beginning of the codon (three nucleotides) for that amino acid. "Hotspot" refers to AID hotspot WRCH/RGYW (W = A/T, R = A/G, H = A/C/T) with the location of the deamination colored in red. "Coldspot" refers to AID coldspot SYC/GRS (S = C/G, Y = C/T) with the location of the unlikely deamination colored in blue. "WA (W = A/T) hotspot" refers to hotspot of Pol η. E-box motif refers to CAGGTG sequences. (C) Flow cytometry sorting strategy for TCR avidity maturation for one (h12) of four clones. Arrows above the graph in indicate that the cells in the indicated gate were taken for an additional SHM and sorting cycle. Cells leading to below the graph indicate that 5000 cells were sorted into groups that were taken for validation and TCR sequencing. Gated on live single cells. The set of three sorting cycles was performed once with four clones ($n = 4$).

Mutations initiated by AID can recruit error prone DNA machinery, which can lead to additional mutations, including Pol η [27,28]. Thus, we maximized for Pol η hotspots, WA, with preference for TA [27,28]. If possible, we would include the E-box motif CAGGTG, important in E47-mediated recruitment of AID [29,30]. Lastly, to maintain high expression we tried to avoid tandem rare codons and maximize the codon adaptation index [31]. After applying this algorithm to the TCR sequence of the hT27 TCR, there was an improvement in a number of aspects for SHM (Fig. 1B).

SHM of hT27 TCR and sorting cycles

We transduced BWZ-8S cells with the hT27 TCR following optimization of the DNA sequence for SHM. To ensure that cells contain only one TCR copy, we used a very low multiplicity of infection (MOI), resulting in about 1% TCR+ cells. We sorted these cells, and induced SHM by adding dox to four clones (h.5, 7, 8, and 12). After 24 days, we sorted cells with increased tetramer binding at a given TCR expression level, indicative of enhanced avidity. The sorted cells underwent a second SHM and sorting cycle in which there were three distinct populations relative to the native low-avidity TCR: no change in avidity, medium-high avidity ("MHA"), and high-avidity ("HA"). The HA population underwent a third SHM and sorting cycle. No further shift in tetramer/TCR ratio was observed, but there were some high-avidity cells with high TCR expression ("HA HiEx"). We sorted 5000 cells from each group, MHA from the second cycle and HA, and among them HA HiEx, from the third cycle (Fig. 1C, Supporting Information Fig. S2). Sorted groups had considerably enhanced tetramer binding than the parental lines (Supporting Information Fig. S3). We also performed a functional TCR activation assay using CPRG but observed no activation, even though this assay works for other TCRs in these cells (data not shown). Regardless, the tetramer binding assays demonstrate that there is an increase in binding avidity, and functional assays will be performed in primary T cells.

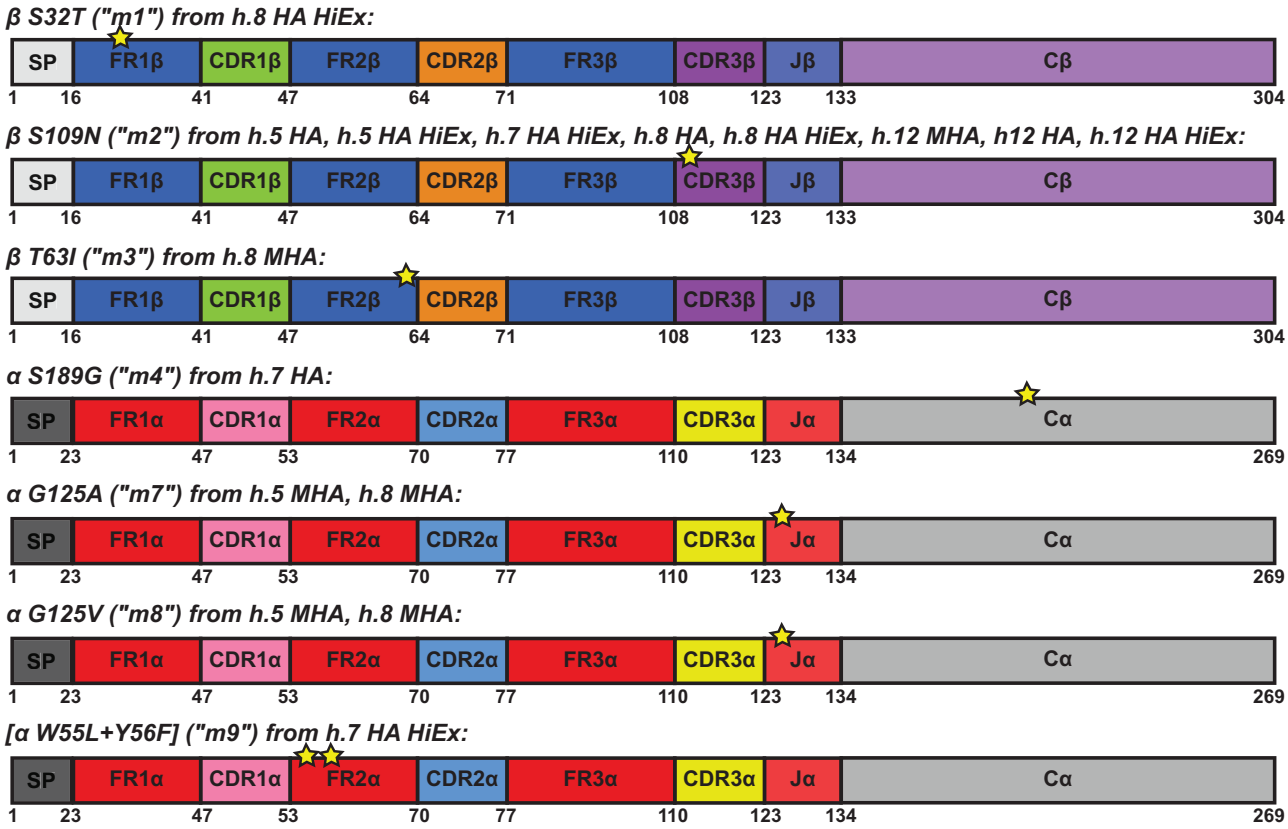

Figure 2. *Mutant hT27 TCRs generated by SHM.* Mutant TCRs identified following SHM using SMRT high-throughput sequencing. Mutations, mutant number designation, and sorted groups in which the mutant TCR was identified are listed above a schematic representation of the TCR sequence. Numbers below the TCR indicate the first amino acid of the region. Length is not to scale. A star indicates the location of the mutation. Domains: C = constant, CDR = complementary determining region, FR = framework region, J = joining. Mutations α W55L and α Y56F, which alone would be designated m5 and m6, occurred as a double mutation designated m9. Results are from a single extraction ($n = 1$) for each of the 12 groups and a single high-throughput sequencing experiment.

Identification of mutations using long-read high throughput sequencing

To identify the mutations responsible for the shift in tetramer binding, we used single-molecule real-time (SMRT) sequencing with Sequel platform [32]. This technology generates long-reads containing the entire 2 kb TCR sequence, allowing us to detect if mutations in distant regions are on the same TCR. The sequencing results were demultiplexed and circular consensus sequences were built from reads with >7 passes of our 2 kb sequence with a predicted accuracy above 99.9%. We identified eight mutant TCRs bearing eight unique missense mutations or one silent mutation, either alone or in combination, from 11 unique DNA mutations (Fig. 2, Supporting Information Tables S1 and S2). One sample, h.12 HA, had few reads due to a technical problem, but Sanger sequencing suggests that nearly all cells in this sample contain the β G326A mutation on the DNA, which leads to β S109N (Supporting Information Fig. S4). All but two mutations were within six bases of the AID hotspot motif, WRCH/DGYW, strongly suggesting that the mutations arose in SHM (Supporting Information Table S2).

TCR expression and enhanced tetramer binding of mutant TCRs

To analyze the effects of the mutations on TCR avidity, we performed several binding and functional assays in primary T cells transduced with the TCRs. Initial screening was performed in primary mouse T cells due to availability. We selected β S109N ("m2"), β T63I ("m3"), α S189G ("m4"), α G125V ("m7"), and α W55L+Y56F ("m9") for further analysis in human T cells from PBMCs) based on the initial screens for IFN-γ production (Supporting Information Fig. S5). The first assay in transduced PBMCs was for binding avidity to tetramers and for TCR expression. The transduced TCRs have a mouse TCR (mTCR) constant region, allowing for detection and gating on transduced PBMCs. All of the mutant hT27 TCRs displayed enhanced tetramer binding compared to the wild-type (WT) TCR (Fig. 3, see also gating strategy in Supporting Information Fig. S6). Mutant m2 was a significantly stronger binder at high and low concentrations. Interestingly, at higher tetramer concentrations all hT27-derived TCRs were stronger binders than T1367. At lower concentrations, there was a trend for m9 to have comparable binding with T1367, and

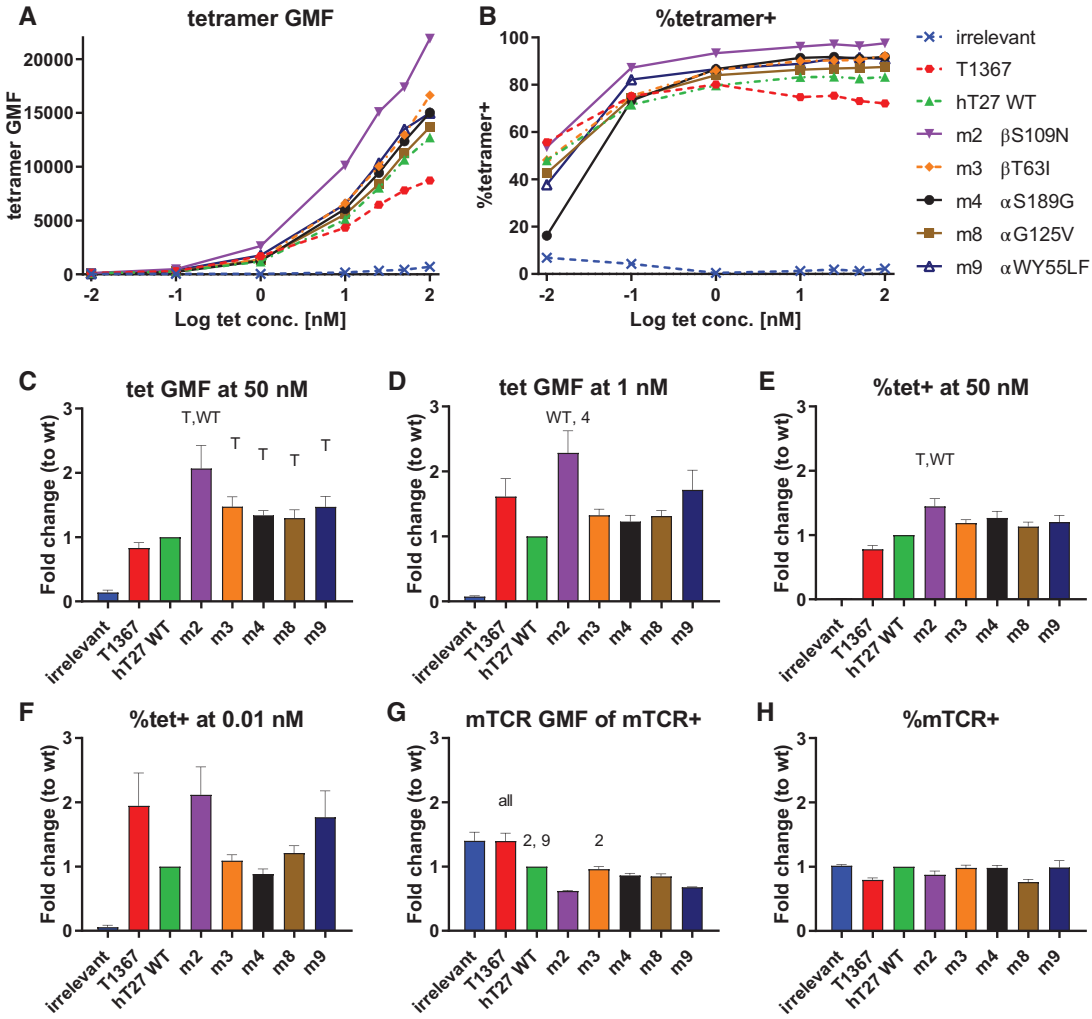

Figure 3. *Tetramer and mTCR staining of TCR-transduced human PBMCs.* Human PBMCs were transduced with TCRs and stained with HLA-A2-MAGE-A1$_{278\text{-}286}$ tetramers and anti-CD4, CD8, mTCRβ. Irrelevant TCR was the Pmel-1 TCR. hT27 mutant TCRs indicated by "m" and then mutant number. All data were collected by flow cytometry. (A) Geometric mean fluorescence (GMF) of tetramer staining. Results in are from a single donor (n = 1) and representative of one of four independent experiments. (B) Percent of tetramer positive cells. Results in are from a single donor (n = 1) and representative of one of four independent experiments. (C–H) Fold change compared to hT27 WT from four independent experiments (n = 4). Multiple comparisons between all groups, excluding the irrelevant TCR, were performed with Tukey's correction following one-way unpaired ANOVA. A statistically significant result ($\alpha = 0.05$) is indicated with a shorthand representation (T = T1367, WT = WT hT27, 2 = m2, 9 = m9, all = all other TCRs) of the group with lower fold change above the bar of the group with higher fold change. (C) GMF of tetramers at a 50 nM concentration. Statistically significant comparisons: m2 > T1367 ($p = 0.0002$), m2 > WT ($p = 0.0144$), m3 > T1367 ($p = 0.0292$), m4 > T1367 ($p = 0.0067$), and m9 > T1367 ($p = 0.0221$). (D) GMF of tetramers at a 50 nM concentration. Statistically significant comparisons: m2 > WT ($p = 0.005$) and m2 > m4 ($p = 0.0271$). (E) %tetramer+ at a 50 nM concentration. Statistically significant comparisons: m2 > T1367 ($p = 0.0009$) and m2 > WT ($p = 0.0042$). (F) %tetramer+ at a 0.01nM concentration. No comparisons were statistically significant. (G) mTCR GMF. Statistically significant comparisons: T1367 > WT ($p = 0.0005$), T1367 > m2 ($p < 0.0001$), T1367 > m3 ($p = 0.0002$), T1367 > m4 ($p < 0.0001$), T1367 > m8 ($p < 0.0001$), T1367 > m9 ($p < 0.0001$), WT > m2 ($p = 0.0009$), WT > m9 ($p = 0.0051$), and m3 > m2 ($p = 0.003$). (H) %mTCR+ cells. No comparisons were statistically significant. (C–H) Error bars represent mean ± SEM. (A–G) Gated on live CD8+mTCRβ+ cells. (H) Gated on all live CD8+ cells. Gating strategy is shown in Supporting Information Fig. S6.

for m3, m4, and m8 to have stronger binding in between T1367 and hT27 WT (Fig. 3C–F). Interestingly, the TCR expression level was significantly higher for T1367 compared to all hT27-derived TCRs, and significantly lower expression for m2 and m9 compared to the WT (Fig. 3G). There were no statistically significant differences in the percent of mTCR positive cells (Fig. 3H). These results show that the mutant TCRs have improved TCR binding avidity compared to the WT, but not due to increased TCR expression levels.

Enhanced cytokine production of mutant TCRs

To begin our functional analysis in transduced human PBMCs, we performed intracellular cytokine staining assays for IFN-γ and IL2. The effective concentration 50% (EC_{50}) is peptide concentration at the halfway between maximal and minimal activity. A low EC_{50} indicates high functional avidity. The EC_{50} of the mutant hT27 TCRs was lower by approximately four orders of magnitude for IFN-γ production (Fig. 4A, see also gating strategy in Supporting

Information Fig. S7) and three for IL2 production compared to the WT (Fig. 4B). The order of functional avidity of IFN-γ production according to EC_{50} (Fig. 4A) was T1367 (EC_{50} = 0.247 pM) > m9 (0.275 pM) > m2 (0.289 pM) > m3 (0.352 pM) > m4 (0.535 pM) > m8 (0.982 pM) >> WT hT27 (3543 pM). It should be that although m2 did not have the lowest EC50 value, it mediated strong cytokine production even with minute quantities of peptide. This trend was the same with IL2 (Fig. 4B). Toward 721.211-A2 cells, which express MAGE-A1 (Supporting Information Fig. S8), the order of activity was m2 (49.7% IFN-γ+) >> T1367 (11%) > m3 (6.9%) > m4 (5.6%) > m9 (5.4%) > m8 (3.8%) > WT (3.3%) (Fig. 4C). All TCRs except for m2 did not show nonspecific activity toward T2 cells with an irrelevant peptide, $MUC1_{13\text{-}21}$, or EL4-HHD cells, which do not express human MAGE-A1 (Fig. 4C). All of the trends in cytokine production were also observed in PBMCs from a second donor (Supporting Information Fig. S9). In CD4+ cells, m2 had reduced nonspecific activity (Supporting Information Fig. S9D), as has been shown with other ultra-high avidity TCRs [7].

Enhanced cytotoxicity of mutant TCRs in transduced T cells

To further study TCR activity for all TCRs that have not lost specificity, all but m2, we performed a cytotoxicity assay. Toward T2 cells loaded with MAGE-$A1_{278\text{-}286}$ peptide, the order of activity was T1367 > m9 > m4 > m8 > m3 > hT27 WT (Fig. 5A). No nonspecific killing above background was observed toward T2 cells loaded with an irrelevant peptide, $MUC1_{13\text{-}21}$ (Fig. 5B). These trends were similar in a second donor, except that m9 and m4 showed higher activity than T1367 toward cells loaded with MAGE-$A1_{278\text{-}286}$, and that m9 appeared to be slightly higher than the others toward cells loaded with $MUC1_{13\text{-}21}$ (Supporting Information Fig. S10). Toward 721.211-A2 cells the order of activity was T1367, m9 > m3 > m4, m8, hT27 WT (Fig. 5C). No nonspecific killing above background was observed toward EL4-HHD cells (Fig. 5D). Taken together with the tetramer and cytokine results, the SHM-generated mutant TCRs display enhanced avidity and activity compared to the WT, although the order among the mutant TCRs was not always consistent.

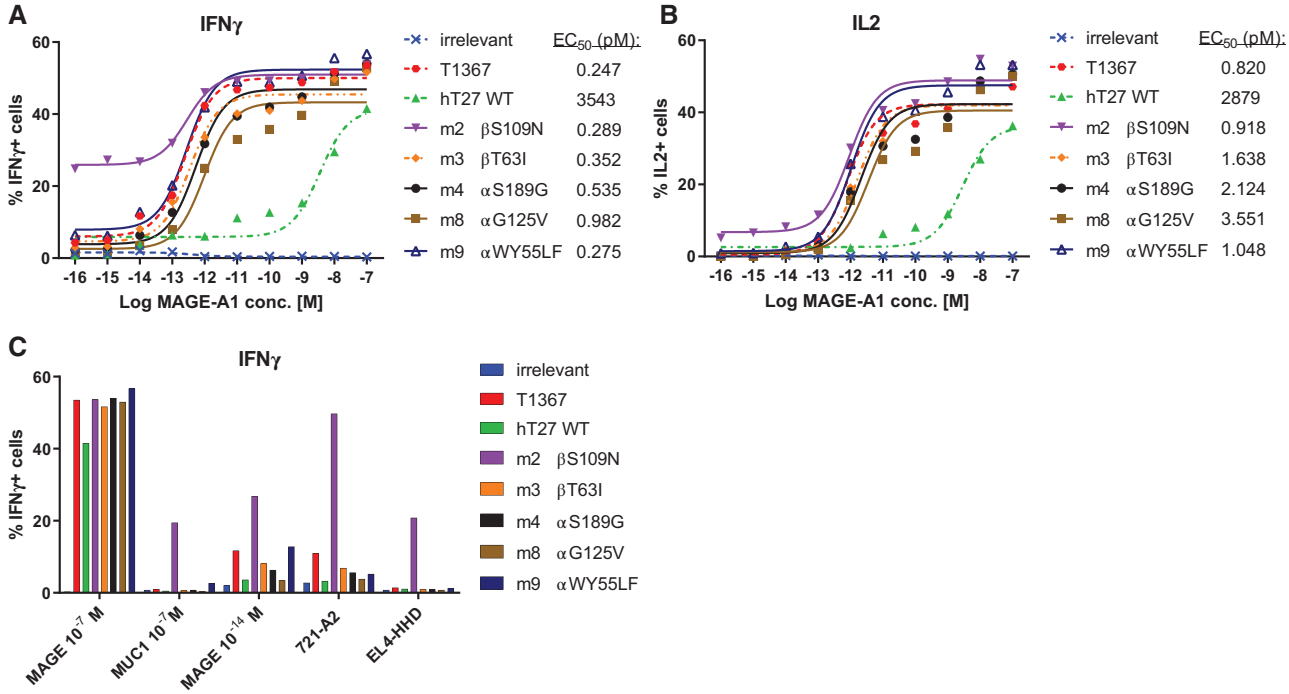

Figure 4. *Intracellular cytokine staining assays with TCR-transduced human PBMCs.* Human PBMCs were transduced with TCRs and co-cultured with target cells for 6 h, with BFA added 2 h into the co-culture to prevent cytokine secretion. Irrelevant TCR was the Pmel-1 TCR. EC_{50} was calculated with nonlinear regression (three-parameter) in GraphPad Prism. All data were collected by flow cytometry. (A) IFN-γ following stimulation with peptide-loaded T2 cells. (B) IL2 following stimulation with peptide-loaded T2 cells. (C) IFN-γ following stimulation with T2 cells loaded with MAGE-A1 or MUC-1 peptide, 721.211-A2 (MAGE-A1+) cells, or EL4-HHD (MAGE-A1-) cells. Gated on live CD8+mTCR+ cells (gating strategy is in Supporting Information Fig. S7). Results are from 1 of 2 donors ($n = 2$, results from the second donor are in Supporting Information Fig. S9) and representative of one of three independent experiments. All assays were performed in duplicates.

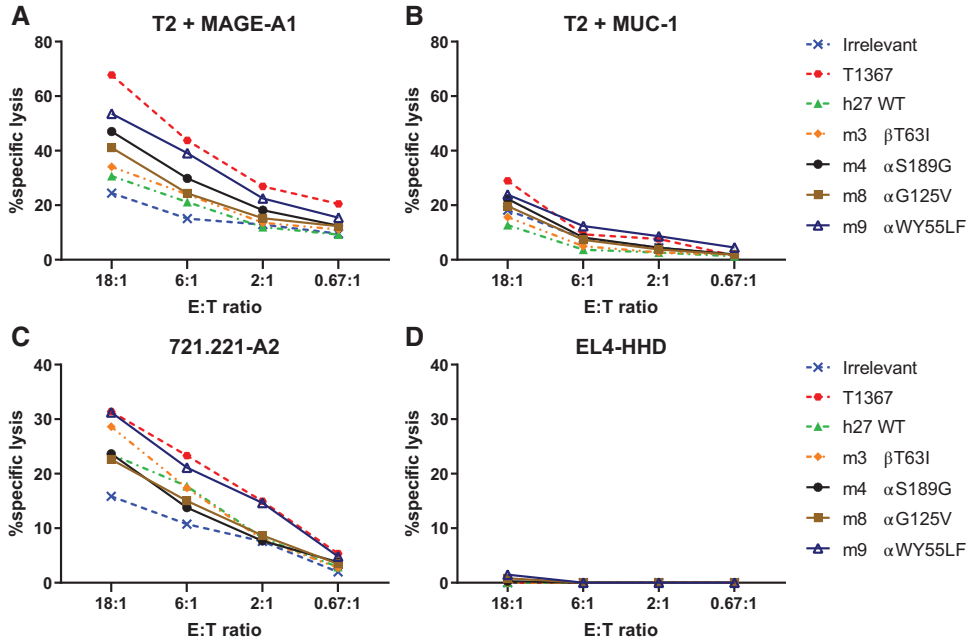

Figure 5. *Cytotoxicity of TCR-transduced human PBMCs*. Human PBMCs were transduced with TCRs and co-cultured with S^{35}-methionine labeled target cells for 5 h at indicated E:T ratios. Cytotoxicity was detected using an S^{35}-methionine release assay. Each graph is with a different target cell. (A) T2 cells loaded with 10 μM MAGE-$A1_{278-286}$ peptide. (B) T2 cells loaded with 10 μM $MUC1_{13-21}$ peptide. (C) 721.211-A2 cells (MAGE-A1+). (D) EL4-HHD cells (MAGE-A–). Results are from one or two donors ($n = 2$, results for the second donor are in Supporting Information Fig. S10) and representative of one of three independent experiments for (A) and (B). Results are from a single donor ($n = 1$) and representative of one of two independent experiments for (C) and (D). Results were normalized by relative number of CD8+mTCR+ cells (determined by flow cytometry). All assays were performed in triplicates.

TCR recognition motif and cross-reactivity of mutants TCRs

To further understand the effects of the mutations of TCR specificity, we performed an alanine screening assay in transduced PBMCs (Fig. 6A). A substitution that leads to a significant reduction (≥75%) can be viewed as part of the recognition motif of the TCR. The observed recognition motif of the mutant TCRs m3, m4, and m9 was xxLEYxxxx. For m8, the recognition motif was xxLEYVxKx. For m2, there was a strong reaction regardless of substitutions. For the WT hT27 TCR, it is difficult to define a motif because there was a substantial reduction with substitutions at the tested peptide concentration in all positions except for p1 and p9. However, it should be noted that changes to the sequence xxLEYVxKx completely abrogated activity (≥95% reduction). In the human proteome, there are 171 peptides containing the xxLEYxxxx motif that are predicted to bind HLA-A2 (Supporting Information Table S3). We screened cross-reactivity to the three strongest predicted binders containing the xxLEYxxxx motif (RTTN, PLOD1, and CD1E), two peptides that contained the xxLEYVxKx sequence (ARHGAP26 and 42) and two highly similar peptides from MAGE-B5 and B16 (Fig. 6B and C). The WT hT27 TCR only displayed cross-reactivity toward ARHGAP42. Mutant m2 reacted with all peptides. Mutants m3, m4, m8, and m9 reacted strongly to 10^{-7}M of ARHGAP42 and moderately to ARHGAP26, MAGE-B5 and 16, and CD1E (Fig. 6B). At a peptide concentration of 10^{-9} M, the cross-reactivity was less severe, but still observed in most cases (Fig. 6C). T1367 only reacted moderately to 10^{-7}M of MAGE-B5 (Fig. 6B), however the recognition motif of T1367 is xxxEYxIKx [10], which is not found in any of these peptides. Mutant TCRs m3, m4, m8, and m9 are less sensitive to substitutions than the WT TCR and have a degree of increased cross-reactivity. However, they have not lost specificity and did not respond to EL4-HHD cells (Figs. 4C and 5D), which express numerous peptides containing the xxLEYxxxx motif [33] (according to RNAseq data from GSM 3022105), including many that are in the human proteome (Supporting Information Table S4).

Structural modeling of hT27 TCR and SHM-generated mutations

To further understand how SHM-generated mutations influence avidity and specificity, we performed structural modeling. TCR-model [34] was used to model the variable regions and we simulated mutations m2, m3, m8, and m9. Mutation m2, β S109N, is in the stem of the CDR3β loop (Fig. 7A). Mutation m3, β T63I, is in the stem immediately before the CDR2β loop (Fig. 7A). Mutation m8, α G125V, is in the hinge between the CDR3α loop and strand of the joining region (Fig. 7B). Mutations in m9, α W55L + α Y56F are soon after the CDR1α loop and they also interact with the stem of the CDR3α loop and core of the alpha chain (Fig. 7B). All of these mutations may

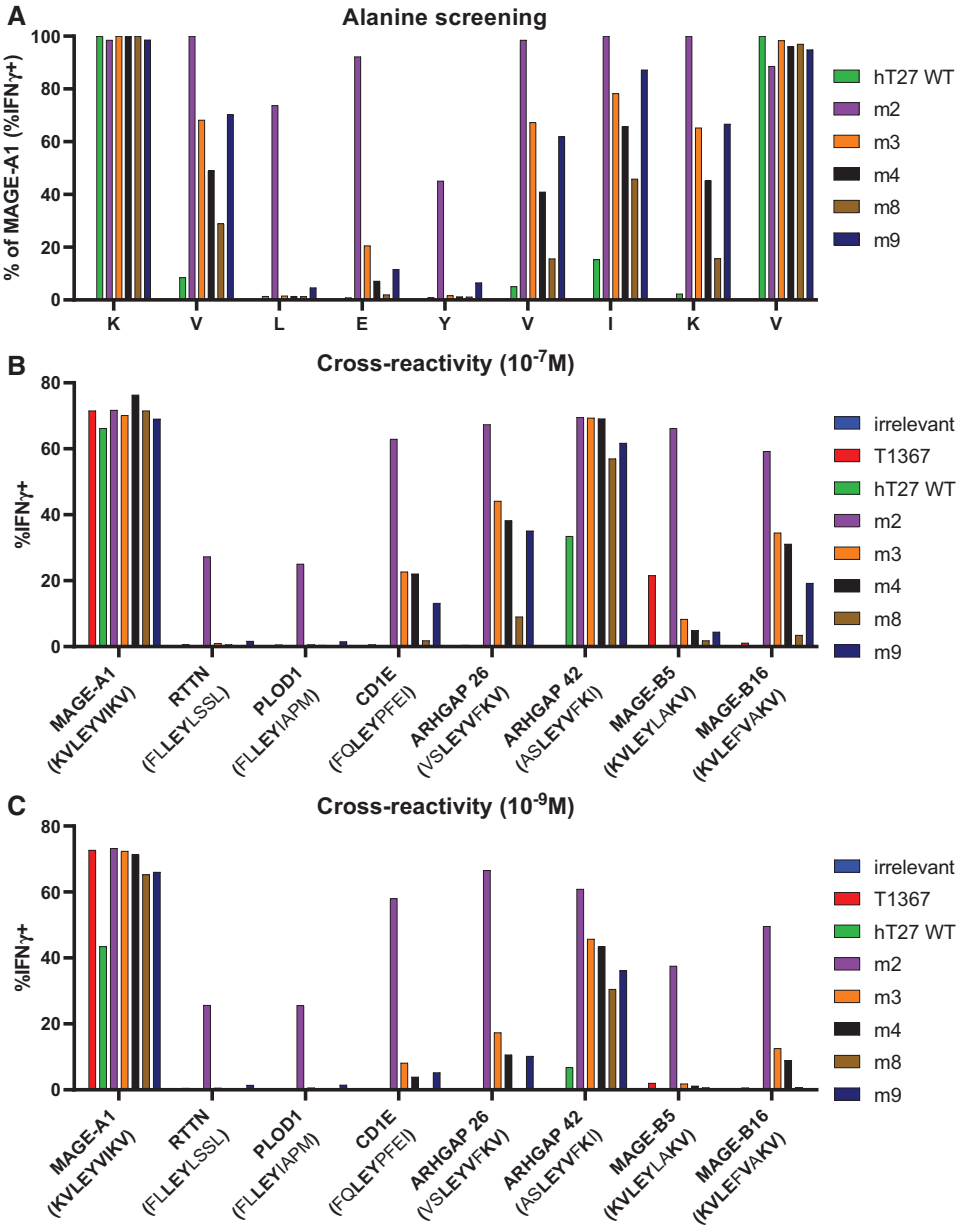

Figure 6. Screening of alanine substitution and potential cross-reactive peptides with TCR-transduced human PBMCs. Human PBMCs were transduced with TCRs and co-cultured with T2 cells loaded the indicated peptide. Co-culture was for 6 h, with BFA added 2 h into the co-culture to prevent cytokine secretion. All data were collected by flow cytometry. (A) Alanine screening at a peptide concentration of 10^{-7}M: Amino acid for the substituted position is listed on the *x*-axis. Percent of activity compared to the native MAGE-A $A1_{278\text{-}286}$ peptide is presented on the *y*-axis (maximum activity capped at 100%). (B and C) Reactivity to MAGE-A1 or several potential cross-reactive peptides containing the xxLEYVxKx motif, xxLEYxxxx motif, or other highly similar peptides. The peptide sequence is listed under the gene with bold letters representing amino acids share with MAGE-$A1_{278\text{-}286}$. (B) Peptide concentration of 10^{-7}M. (C) Peptide concentration of 10^{-9}M. Results are from a single donor ($n = 1$) and each library was screened once. All assays were performed in duplicates. Gated on live CD8+mTCR+ cells (gating strategy is in Supporting Information Fig. S7).

influence the flexibility/conformation of the CDR loops, among additional potential effects. Our TCR contains murine constant regions, so we were able to analyze the known structure of the mouse 2C TCR [35] and simulate the m4 mutation. Mutation m4, α S189N (the equivalent of 175 on the 2C TCR), is in the DE loop of the Cα domain (Fig. 7C), which interacts with CD3 [36].

Discussion

In this study, we have furthered the technology of SHM-driven evolution of TCR avidity, and successfully used it on a clinically relevant TCR, hT27. We focused on five mutant TCRs, bearing six of the eight identified mutations, m2 (β S109N), m3 (β T63I), m4 (α S189G), m8 (α G125V), and m9 (α W55L+Y56F). These

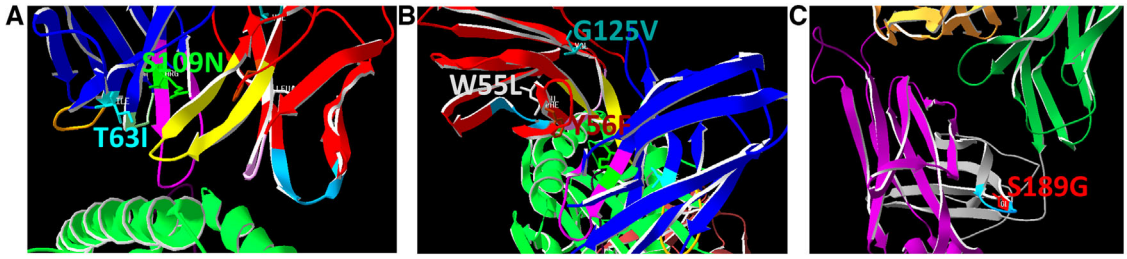

Figure 7. *Structural model of the hT27 TCR with simulated mutations.* (A and B) Structural model for the variable regions was built using TCR model. Region colors: Alpha chain: red, CDR1α: pink, CDR2α: light blue, CDR3α: yellow. Beta chain: blue. CDR1β: light green, CDR2β: orange, CDR3β: purple. MHC (green) and peptide (dark purple) are from the 2YPL (PDB) structure, which contains HLA-B*5703 MHC-I, KF11 peptide from HIV, and the AGA1 TCR. Mutations: m2 (βS102N) in green; m3 (βT63I) in cyan; m8 (αG125V) in turquoise; m9 (αW55L+Y56F) in gray and brown, respectively. (A) Rotated to highlight m2 and m3 on the beta chain. (B) Rotated to highlight m8 and m9 on the alpha chain. (C) Constant regions of hT27 TCR are from a mouse TCR. The structure of the 2C TCR (PDB ID: 1TCR) was used to visualize the mutation m4. Colors: Alpha chain: variable region: green, constant region: light gray, DE loop: light blue, mutation m4 (αS189G) in red. Beta chain: variable region: orange, constant region: magenta.

mutations all enhanced TCR activity compared to the WT hT27 TCR in several in vitro assays. These mutations enhanced TCR avidity, although we did not perform an affinity test using soluble TCRs. Thus, it is unclear if the improved avidity was due to increased affinity or other factors. It would be valuable in future studies to measure affinity to further understand how they improved TCR avidity and function. Interestingly, none of the mutations were to residues that directly interact with the antigen, but several likely influence the flexibility or conformation of the CDR loops or TCR. Aside from m2, the mutant TCRs did not lose specificity.

Potential cross-reactivity toward antigens expressed on vital tissues is a major concern with TCR gene therapy. Mutant TCRs m3, m4, m8, and m9 were less sensitive to changes in the peptide in an alanine screening assay and showed cross-reactivity to peptides that generated no response from the WT, especially at 10^{-7} M (Fig. 6). On the other hand, we observed no response toward EL4-HHD cells (Figs. 4C and 5D), which express many peptides that contain the xxLEYxxxx motif [33] (Supporting Information Table S4). This would seem to indicate that the cross-reactivity to "off-target" peptides is not significant enough to lead to broad cross-reactivity toward all cells. However, it is unclear if there are certain healthy cells that express particular "off-target" peptides at sufficiently high levels to generate a response from the mutant TCRs that can lead to toxicities. It is possible that there would not be substantial cross-reactivity to healthy cells.

It should be noted that the assays used to test specificity and cross-reactivity in this study are quite limited. The alanine screening and follow-up assays test peptides with sequence similarity, not structural similarity. Also, we only tested seven such peptides. Additionally, we only tested reactivity toward a single MAGE-A1-negative cell line, EL4-HHD, which is a mouse cell line. Therefore, it is critical to thoroughly examine cross-reactivity with PBMCs from multiple donors before proceeding with the identified mutant TCRs to clinical trials. This examination can include testing reactivity to all potential cross-reactive peptides. If there are peptides that generate a strong response, absence of processing would need to be demonstrated using an HLA-A2 positive human cell line that overexpress the respective gene. Additionally, wide panels of HLA-A2 positive human tissues and/or cell lines from various tissues can be screened. Also, the most promising TCRs should be tested in vivo in mice before proceeding to clinical trials. It would be recommended to test m3, m4, m8, and m9. The TCR that is most potent and proven safe would be the lead candidate for a clinical setting. If proven safe and effective in vivo, the mutant TCRs generated in this study can potentially be used for cancer immunotherapy.

The mutant TCRs generated in this study were far stronger than the WT hT27 TCR, and were often comparable to T1367. However, T1367 often slightly outperformed the mutant TCRs. This highlights the advantages of the in vivo vaccination approach used to generate T1367 [10], which is highly effective is generating TCRs with affinity in the optimal window. Still, there are some advantages to in vitro methods to enhance TCR affinity, such as SHM. In vitro systems are generally quicker, cheaper, less laborious, and more flexible than in vivo vaccination. Also, with SHM there is a possibility to generate beneficial and potentially broadly applicable mutations in nonhypervariable regions of the TCR. Ultimately, both in vivo and in vitro approaches are legitimate methods to obtain suitable TCRs for immunotherapy.

We did not directly compare SHM to other in vitro techniques for generating TCRs with high affinity/avidity. A detailed comparison of the qualities of SHM and common existing approaches such as random mutagenesis small regions followed by screening in phage [11,37], yeast [12,38], or mammalian cell display [13,39,40] has been discussed previously [14]. In short, some of the key advantages of SHM are that it targets all regions of the TCR, multiple cycles can be performed in the same cells, and it is in a T-cell line without a limit on library size. Disadvantages include that SHM cannot be directed toward particular regions or amino acids if desired and is unlikely to mutate bases that are far from AID hotspots. There are additional methods to obtain high-avidity TCRs, however it is beyond the scope of this discussion to address all of them. Every approach has advantages and limitations, and the selection of an approach will differ according to the goals and restrictions of a study.

All of the mutations in this study apart from m2 are in nonhypervariable regions, which highlights the ability of SHM to

generate widely applicable mutations. Mutant m4 (α S189G on hT27, corresponding to position 58 on TRAC*01) is in the mouse constant region, which is shared with many TCRs. Future studies can test if the avidity enhancement of these mutations is specific to the hT27 TCR or more broadly applicable to other TCRs.

In this study, we used SHM in BWZ.36-drevied cells containing mouse CD8α and the highly active AID mut7.3 [25]. We also built parallel systems with either human CD8α, human CD4, or without CD8 and CD4, together with either the native AID or AID mut7.3. We have not extensively tested SHM in these systems, however they may be suitable for some TCRs in future studies. All of these systems are a step forwards from the previously described 293TREx system [14]. The current system was quicker and had a much higher proportion of beneficial mutations. Additionally, although for the hT27 TCR the functional TCR activation assay with CPRG did not work, this assay does work with other TCRs in BWZ.36-derived cells.

SHM in a T-cell line may be used to improve other forms of immunotherapy aside from TCR gene therapy. Chimeric antigen receptors (CARs) can be also be used to redirect T cells to target cancer. A CAR consists of an antibody fragment that recognizes a cell-surface antigen on tumor cells, as well as T-cell costimulatory and signaling domains. The affinity of a CAR can often be optimized to enhance the therapeutic potential. For example, lowering affinity of CARs that recognize Erbb2 or EGFR has been shown to allow CAR-T cells to kill tumor cells that overexpress the antigen, yet spare healthy cells with normal expression levels [41]. SHM in BWZ.36-derived cells can both generate a library of CARs with different affinities and test the function of the CARs. Currently, these two processes are completely separated. Furthermore, SHM should be well suited for CARs, as it is the natural mechanism to optimize the affinity of the antibodies from which CARs are built. We hope that directed evolution with SHM will be used to improve both TCRs and CARs for cancer immunotherapy.

Materials and Methods

Plasmids and cloning

The cloning of the pBABE-CD3 and pcDNA4-Tet-hAID was described previously [14]. The pCL-Ampho vector was a kind gift from Prof. Haim Cohen (Bar Ilan University, Ramat Gan, Israel). The pCL-Eco and codon-optimized pMSGV1-Pmel-1 TCR vector (codon optimized Pmel-1α and β chains separated by a T2A segment) vector were a kind gift from Dr. Nick Restifo (NIH, Bethesda, MD, USA), as previously described [42]. The codon-optimized MP71-hT27 TCR and MP71-T1367 TCR vectors containing mouse constant regions were a kind gift from Prof. Thomas Blankenstein (MDC, Berlin, Germany), as previously described [10]. The mutant MP71-hT27 TCR vectors and pcDNA4-Tet-hAID mut 7.3 vector, as previously described [25], were generated using site-directed mutagenesis (SDM) with the Phusion SDM Kit (Thermo-Fischer Scientific, Waltham, MA, USA) according to the manufacturer's protocol. The pCDNA6-TR vector, containing the TetR (or TR), was purchased commercially (Invitrogen, Carlsbad, CA, USA). The pMSGV1-TetR vector was generated using restriction-free cloning, as previously described [43], with the Phusion HSII HF polymerase (Thermo-Fischer Scientific) according to the manufacturer's protocol. Sequencing primers: MP71 For: ATTTGTCTGAAAATTAGCTCGA, MP71 Rev: AGAGCAACTACAGCTACTGC, hT27 internal For: CATTTAAATGTATACCCAAATCAA, pMSGV1 For: CCTCAAAGTAGACGGCATCG (Sigma-Aldrich, Rehovot, Israel).

Cell lines

Phoenix-ampho and Platinum-Eco (Plat-E) cells were cultured in "cDMEM" containing DMEM (GibcoBRL, Grand Island, NY, USA) supplemented with 10% FCS (GibcoBRL), 200 mM L-glutamine, 100 mM sodium pyruvate, 1× nonessential amino acids, and 50 μg/mL gentamicin (all Biological Industries, Beit Ha-emek, Israel). 721.211-A2, BWZ.36, DLD1, EL4-HHD, and T2 cells were cultured in "cRPMI" containing RPMI 1640 (GibcoBRL) supplemented with 10% FCS, 200 mM L-glutamine, 100 mM sodium pyruvate, 1× nonessential amino acids, 50 μg/mL gentamicin, and 50 μM β-mercaptoethanol. 721.221-A2 cells are LCL-721.221 cells previously transfected with HLA-A2, because they do not naturally express HLA-I molecules [44]. EL4-HHD cells are EL4 cells from a mouse lymphoma that were stably transfected with an β_2m-HLA-A2-D^b single chain molecule (HHD) [45]. Human PBMCs were cultured in cRPMI supplemented with 300 U/mL rh-IL-2 (ProSpec, Ness Tziona, Israel). Cell lines were all checked for mycoplasma using the EZ-PCR Mycoplasma Test Kit (Biological Industries), and were all found to be negative. Cell lines were generally used between 1 week and 1 month after thawing.

Flow cytometry and FACS

For flow cytometry cells were stained with antibodies for 30 min at 4°C using the dilution recommended by the manufacture, unless indicated otherwise in parenthesis. Anti-mouse APC-CD3 and anti-human APC-IFNγ, FITC-CD8 (1:100), PE-Cy7-IL2 (1:50), and PerCP-eFlour710-CD4 (1:100) antibodies were purchased from eBioscience (San Jose, CA, USA), and anti-mouse PE-TCRβ (1:333) from BioLegend (San Diego, CA, USA). Viability staining was performed with either Zombie-aqua (1:500, BioLegend) for cells to be fixed and permeabilized, or 1 μM DAPI (BioLegend) for other cells. APC-conjugated HLA-A2-MAGE-$A1_{278\text{-}286}$ were prepared by combining biotinylated monomers from the NIH tetramer facility (Bethesda, MD, USA) and APC-Streptavadin (eBioscience) mixed at a 4:1 molar ratio. APC-Streptavadin was added to the monomers in five portions separated by 20 min. Cells were stained with tetramers for 1 h at 4°C using a 1:200 dilution unless otherwise noted, and then stained with antibodies. BWZ-derived cells were sorted via FACS using a 100 μm nozzle,

with 100 nM DAPI added immediately before running. All results were analyzed using FlowJo software (ThreeStar, San Carlos, CA, USA). Flow cytometry was performed in accordance with journal guidelines [46].

Electroporations

BWZ.36-derived cells were electroporated with 5 μg of linearized DNA for 2 ms at 400 V with the ECM 830 electroporator (BTX, Hollistone, MA, USA) at a density of 2×10^7 cells/mL in Opti-MEM (GibcoBRL), 250 μL (5×10^6 cells) per 4 mm cuvette. Selection of cells with stable expression of TetR (on the pCDNA6-TR vector) was performed for 2 weeks using 6 μg/mL blastidin (Invitrogen). Subsequently, selection of cells with stable expression of AID or AID mut 7.3 (on the pCDNA4 vector) was performed for 2 weeks using 600 mg/mL zeocin (Invitrogen). Cells were maintained in 3 μg/mL blastidin and 300 mg/mL zeocin. Following SHM selection antibiotics were not added to the medium.

RNA extraction and reverse transcriptase (RT)-PCR

RNA was extracted from cells using the RNeasy Mini kit (Qiagen, Hilden, Germany). RT-PCR to generate cDNA from mRNA was performed with the Tetro RT-PCR kit (Bioline, London, UK) using oligo-dT primers. Gene expression from cDNA was performed using PCR with gene-specific primers. AID For: ATGGACAGCCTCTTGATG, AID Rev: TCAAAGTCCCAAAGTACG, TetR For: CGTAAACTCGCCCAGAAG, TetR Rev: AGTAAAATGCCCCACAGCG, mGAPDH For: CGTGTTCCTACCCCCAATGT, mGAPDH Rev: TGTCATCATACTTGGCAGGTTTCT. MAGE-A1 For: CAACTTCACTCGACAGAGGCA, MAGE-A1 Rev: CCTAGGCAGGTGACAAGGAC. hGAPDH For: TCACCAGGGCTGCTTTTAACT, hGAPDH Rev: GCCATGGGTGGAATCATATTGG. All primers were synthesized by Sigma-Aldrich.

Retroviral transductions

Retroviruses were produced in Phoenix-ampho cells for transduction of human PBMCs or Plat-E cells for transduction of mouse BWZ.36-derived cells. Cells were seeded on 6-well plates, 8×10^5 cells/well, grown to 70–90% confluence, and transfected with 1.5 μg of the target vector and 0.5 μg pCL-Ampho (gag/pol/ampho-env) using Lipofectamine2000 (Invitrogen). The supernatant containing viruses was harvested 42 h posttransfection and cell debris was removed with 0.45 μm filters.

Human PBMCs were isolated from leukocyte samples from the Magen David Adom blood bank (Ramat Gan, Israel) using Ficoll-Paque (GE Healthcare, Chicago, IL, USA) and frozen in aliquots of 2×10^7 cells/vial. PBMCs were thawed, washed, and suspended in cRPMI supplemented with 50 ng/mL anti-human CD3ε (eBioscience, clone OKT-3) and 300 U/mL rh-IL2. Cells were seeded at a density of 2×10^6 cells/mL, 1mL per well of a 24-well plate, and incubated for 40 h at 37°C. Nontissue culture plates were coated with retronectin (Takara Bio, Otsu, Japan), viruses were added, 2 mL per well, plates were centrifuged at 2000 *g* for 2 h at 32°C without brakes, and 1.5 mL of supernatant was removed. Activated PBMCs were added, 1×10^6 cells in 1.5 mL per well, and centrifuged at 1500 rpm for 10 min without brakes.

BWZ.36-derived cells were transduced in 24-well plates by mixing 4×10^5 cells in 200 μL with 1 mL of viruses (undiluted or with the indicated dilution of viruses) in the presence of 4 μg/mL protamine sulfate (Sigma-Aldrich). Plates were centrifuged at 1000 *g* for 1.5 h at 32°C without brakes and incubated overnight. Selection of cells with stable expression of CD3 (on the pBABE-CD3 vector) was performed for 2 weeks using 0.5 μg /mL puromycin (Invitrogen).

SHM and sorting cycles to select avidity-enhanced hT27 TCRs

SHM-ready BWZ-derived cells were transduced with the hT27 TCR and sorted, one cell per well. SHM was initiated by adding doxycline ("dox"; Sigma-Aldrich), an analog of tetracycline, at a concentration of 1 μg/mL following expansion and selection of clones based on mTCRβ expression. After 24 days cells with an increased tetramer/TCR staining ratio were sorted. Additional SHM cycles were 10–14 days of incubation with dox followed by sorting, 5000 cells per well. After two or three total cycles, cells were sorted into a number of groups for sequencing and avidity analysis.

High-throughput SMRT sequencing with PacBio Sequel system

Genomic DNA (gDNA) was extracted using the DNeasy Blood & Tissue kit (Qiagen). hT27 TCR was amplified from gDNA using the Phusion Hotstart II HF polymerase. Primers contained a tag (underlined), 8N unique molecular identifiers (UMIs), and an MP71 specific sequence (uppercase). For: gactgtacagtgatcgtacgnnnnnnnnTCCAAGCTCACTTACAGGCGG, Rev: ctgatcgatcgtcaactagcnnnnnnnnTGGCGGTAAGATGCTCGAATTC (Sigma-Aldrich) were used for the first two PCR cycles to add UMIs. The product was purified and amplified with primers of the underlined tag for 35 PCR cycles. The final product was purified with PacBio AMPure beads, library prepared with the SMRTbell barcoded adapter kit, and samples run on a PacBio Sequel System (Pacific Biosciences, Menlo Park, CA, USA). For analysis, demultiplexing followed by circular consensus sequence analysis was performed using SMRT Link v5.0, and further analysis in UNIX using bwa and samtools, and mutations were visualized using the Integrated Genomics Viewer.

Peptide-loading of T2 cells for in vitro functional assays

T2 cells were pulsed with the indicated peptides at the indicated concentrations for 2 h in Opti-MEM. MAGE-A1$_{278-286}$ (KVLEYVIKV) and MUC1$_{13-21}$(LLLTVLTVV) peptides with >99% purity were synthesized by Sigma-Aldrich. Crude peptides for MAGE-A1$_{278-286}$ (KVLEYVIKV), alanine substitution library, and potential cross-reactive peptides were synthesized by Genemed Synthesis (San Antonio, TX, USA).

In vitro cytokine production assay detected by intracellular staining

IFN-γ and IL2 production was detected by intracellular staining. Transduced PBMCs, 1.5×10^5 per well, were co-cultured with target cells, 1×10^5 per well, for 6 h at an E:T (Effector:Target) ratio of 1.5:1. Brefeldin A ("BFA"; eBioscience) was added 2 h into the co-culture for prevention of cytokine secretion. Cells were then stained for viability with Zombie-aqua, fixed, permeabilized, and stained for hCD4, hCD8, hIL2, hIFN-γ, and mTCRβ and analyzed by flow cytometry. Assays were performed in duplicates.

In vitro cytotoxicity assay

In vitro cytotoxicity was evaluated with a S^{35}-methionine release assay. Target cells were labeled with S^{35}-methionine (PerkinElmer, Waltham, MA, USA) overnight. Transduced PBMCs were then co-cultured with target cells, 5×10^3 per well, for 5 h at indicated E:T ratios. Target cells alone were used for spontaneous release, and 50mM NaOH was added for total release. Plates were then centrifuged, 50 μL of the supernatant was transferred to a new plate, and 150 μL MicroScint 40 (PerkinElmer) was added to each well. S^{35}-methionine released into the medium due to specific tumor lysis was detected with a Micro β counter (PerkinElmer). Percent specific lysis was calculated as 100 × (sample release − spontaneous release)/(total release − spontaneous release). If sample release was lower than spontaneous release, it was considered that there was no killing. Assays were performed in triplicates.

Structural modeling

The structural model for the variable regions of the hT27 TCR was built using TCRmodel, as previously described [34]. The orientation of TCR chains and MHC was derived from the AGA1 TCR (PDB ID: 2YPL) structure, which contains HLA-B*5703 MHC, KF11 peptide from HIV, and the AGA1 TCR. The structural model for murine constant regions of hT27 TCR was taken from the structure of the mouse 2C TCR (PDB ID: 1TCR). Mutations were simulated using Swiss-PDB Viewer (Swiss Institute of Bioinformatics, Lausanne, Switzerland).

Statistical analysis

Statistical analysis was performed using GraphPad Prism 6.0. All multiple comparisons following ANOVA used Tukey's correction for honest significant difference. EC_{50} values were calculated on log10-transformed values with nonlinear regression of log (agonist) versus response (three parameters). All *p*-values are two-sided and following Tukey's correction.

Acknowledgements: We would like to thank all those who provided plasmids and cell lines, as mentioned above. We would like to thank Prof. Thomas Blankenstein for the TCR vectors and general guidance. We would like to thank Prof. Cyrille Cohen for guidance regarding transduction of human PBMCs. We would like to thank Stacy Davis for assisting in culturing hT27 TCR-transduced BWZ cell lines. This work was funded by Israel Science Foundation (grant No. 496/14, principal funding recipient: Lea Eisenbach).

Conflict of interests: DB, YG, ET, EG, NF, and LE are listed as inventors in a pending patent. The authors disclose no further commercial or financial conflicts of interest.

Peer review: The peer review history for this article is available at https://publons.com/publon/10.1002/eji.202049007.

Data availability statement: The data that support the findings of this study are openly available in figshare at http://doi.org/10.6084/m9.figshare.12803501.

References

1 **Goldrath, A. W. and Bevan, M. J.**, Selecting and maintaining a diverse T-cell repertoire. *Nature*. 1999. **402**: 255–262.

2 **Rosenberg, S. A., Restifo, N. P., Yang, J. C., Morgan, R. A. and Dudley, M. E.**, Adoptive cell transfer: a clinical path to effective cancer immunotherapy. *Nat. Rev. Cancer.* 2008. **8**: 299–308.

3 **Kershaw, M. H., Westwood, J. A., Slaney, C. Y. and Darcy, P. K.**, Clinical application of genetically modified T cells in cancer therapy. *Clin. Transl. Immunol.* 2014. **3**: e16.

4 **Michielin, O., Rufer Schumacher, N., Romero, P., Speiser, D. E., Raquel Gomez-Eerland, V., Thome, M., M Michael Hebeisen, T. N. et al.**, Delimiting maximal CD8 T cell function evidence for a TCR affinity threshold evidence for a TCR affinity threshold delimiting maximal CD8 T cell function. *J. Immunol.* 2010. **184**: 4936–4946.

5 **Irving, M., Zoete, V., Hebeisen, M., Schmid, D., Baumgartner, P., Guillaume, P., Romero, P. et al.**, Interplay between T cell receptor binding kinetics and the level of cognate peptide presented by major histocompatibility complexes governs CD8+ T cell responsiveness. *J. Biol. Chem.* 2012. **287**: 23068–23078.

6 **Holler, P. D., Chlewicki, L. K., Kranz, D. M.**., TCRs with high affinity for foreign pMHC show self-reactivity. *Nat. Immunol.* 2003. **4**: 55–62.

7 **Zhao, Y., Bennett, A. D., Zheng, Z., Wang, Q. J., Robbins, P. F., Yu, L. Y. L., Li, Y. et al.**, High-affinity TCRs generated by phage display provide CD4+ T cells with the ability to recognize and kill tumor cell lines. *J. Immunol.* 2007. **179**: 5845–5854.

8 **Hogquist, K. A., Baldwin, T. A. and Jameson, S. C.**, Central tolerance: learning self-control in the thymus. *Nat. Rev. Immunol.* 2005. **5**: 772–782.

9 **Aleksic, M., Liddy, N., Molloy, P. E., Pumphrey, N., Vuidepot, A., Chang, K.-M. and Jakobsen, B. K.**, Different affinity windows for virus and cancer-specific T-cell receptors: implications for therapeutic strategies. *Eur. J. Immunol.* 2012. **42**: 3174–3179.

10 **Obenaus, M., Leitão, C., Leisegang, M., Chen, X., Gavvovidis, I., van der Bruggen, P., Uckert, W. et al.**, Identification of human T-cell receptors with optimal affinity to cancer antigens using antigen-negative humanized mice. *Nat. Biotechnol.* 2015. **33**: 402–407.

11 **Li, Y., Moysey, R., Molloy, P. E., Vuidepot, A.-L., Mahon, T., Baston, E., Dunn, S. et al.**, Directed evolution of human T-cell receptors with picomolar affinities by phage display. *Nat. Biotechnol.* 2005. **23**: 349–354.

12 **Holler, P. D., Holman, P. O., Shusta E, V., O'Herrin, S., Wittrup, K. D. and Kranz, D. M.**, In vitro evolution of a T cell receptor with high affinity for peptide/MHC. *Proc. Natl. Acad. Sci. U. S. A.* 2000. **97**: 5387–5392.

13 **Chervin, A. S., Aggen, D. H., Raseman, J. M. and Kranz, D. M.**, Engineering higher affinity T cell receptors using a T cell display system. *J. Immunol. Methods.* 2008. **339**: 175–184.

14 **Bassan, D., Gozlan, Y. M., Sharbi-Yunger, A., Tzehoval, E. and Eisenbach, L.**, Optimizing T cell receptor avidity with somatic hypermutation. *Int. J. Cancer.* 2019. https://doi.org/10.1002/ijc.32612.

15 **Luo, Z., Ronai, D. and Scharff, M. D.**, The role of activation-induced cytidine deaminase in antibody diversification, immunodeficiency, and B-cell malignancies. *J. Allergy Clin. Immunol.* 2004. **114**: 726–735; quiz 736.

16 **Rogozin, I. B. and Diaz, M.**, Cutting edge: DGYW/WRCH is a better predictor of mutability at G:C bases in Ig hypermutation than the widely accepted RGYW/WRCY motif and probably reflects a two-step activation-induced cytidine deaminase-triggered process. *J. Immunol.* 2004. **172**: 3382–3384.

17 **Robbins, P. F., Morgan, R. A., Feldman, S. A., Yang, J. C., Sherry, R. M., Dudley, M. E., Wunderlich, J. R. et al.**, Tumor regression in patients with metastatic synovial cell sarcoma and melanoma using genetically engineered lymphocytes reactive with NY-ESO-1. *J. Clin. Oncol.* 2011. **29**: 917–924.

18 **Rapoport, A. P., Stadtmauer, E. A., Binder-Scholl, G. K., Goloubeva, O., Vogl, D. T., Lacey, S. F., Badros, A. Z. et al.**, NY-ESO-1-specific TCR-engineered T cells mediate sustained antigen-specific antitumor effects in myeloma. *Nat. Med.* 2015. **21**: 914–921.

19 **Linette, G. P., Stadtmauer, E. A., Maus, M. V., Rapoport, A. P., Levine, B. L., Emery, L., Litzky, L. et al.**, Cardiovascular toxicity and titin cross-reactivity of affinity-enhanced T cells in myeloma and melanoma. *Blood*. 2013. **122**: 863–871.

20 **Morgan, R. A., Chinnasamy, N., Abate-Daga, D., Gros, A., Robbins, P. F., Zheng, Z., Dudley, M. E. et al.**, Cancer regression and neurological toxicity following anti-MAGE-A3 TCR gene therapy. *J. Immunother.* 2013. **36**: 133–151.

21 **Weon, J. L. and Potts, P. R.**, The MAGE protein family and cancer. *Curr. Opin. Cell Biol.* 2015. **37**: 1–8.

22 **Ottaviani, S., Zhang, Y., Boon, T. and van der Bruggen, P.**, A MAGE-1 antigenic peptide recognized by human cytolytic T lymphocytes on HLA-A2 tumor cells. *Cancer Immunol. Immunother.* 2005. **54**: 1214–1220.

23 **Sanderson, S. and Shastri, N.**, LacZ inducible, antigen/MHC-specific T cell hybrids. *Int. Immunol.* 1994. **6**: 369–376.

24 **Cafri, G., Sharbi-Yunger, A., Tzehoval, E. and Eisenbach, L.**, Production of LacZ inducible T cell hybridoma specific for human and mouse $gp100_{25-33}$ peptides. Cobbold M, *PLoS One*. 2013. **8**: e55583.

25 **Wang, M., Yang, Z., Rada, C. and Neuberger, M. S.**, AID upmutants isolated using a high-throughput screen highlight the immunity/cancer balance limiting DNA deaminase activity. *Nat. Struct. Mol. Biol.* 2009. **16**: 769–776.

26 **Zheng, N.-Y., Wilson, K., Jared, M. and Wilson, P. C.**, Intricate targeting of immunoglobulin somatic hypermutation maximizes the efficiency of affinity maturation. *J. Exp. Med.* 2005. **201**. 1467–1478.

27 **Rogozin, I. B., Pavlov, Y. I., Bebenek, K., Matsuda, T. and Kunkel, T. A.**, Somatic mutation hotspots correlate with DNA polymerase ||[eta]| error spectrum. *Nat. Immunol.* 2001. **2**: 530–536.

28 **Pavlov, Y. I., Rogozin, I. B., Galkin, A. P., Aksenova, A. Y., Hanaoka, F., Rada, C. and Kunkel, T. A.**, Correlation of somatic hypermutation specificity and A-T base pair substitution errors by DNA polymerase eta during copying of a mouse immunoglobulin kappa light chain transgene. *Proc. Natl. Acad. Sci. U. S. A.* 2002. **99**: 9954–9959.

29 **Michael, N., Shen, H. M., Longerich, S., Kim, N., Longacre, A. and Storb, U.**, The E box motif CAGGTG enhances somatic hypermutation without enhancing transcription. *Immunity*. 2003. **19**: 235–242.

30 **Tanaka, A., Shen, H. M., Ratnam, S., Kodgire, P. and Storb, U.**, Attracting AID to targets of somatic hypermutation. *J. Exp. Med.* 2010; **207**: 405–415.

31 **Scholten, K. B. J., Kramer, D., Kueter, E. W. M., Graf, M., Schoedl, T., Meijer, C., Schreurs, M. W. J. et al.**, Codon modification of T cell receptors allows enhanced functional expression in transgenic human T cells. *Clin. Immunol.* 2006. **119**: 135–145.

32 **Rhoads, A. and Au, K. F.**, PacBio sequencing and its applications. *Genomics Proteomics Bioinform.* 2015. **13**: 278–289.

33 **Laumont, C. M., Vincent, K., Hesnard, L., Audemard, É., Bonneil, É., Laverdure, J. P., Gendron, P. et al.**, Noncoding regions are the main source of targetable tumor-specific antigens. *Sci. Transl. Med.* 2018. **10**. https://doi.org/10.1126/scitranslmed.aau5516.

34 **Gowthaman, R. and Pierce, B. G.**, TCRmodel: high resolution modeling of T cell receptors from sequence. *Nucleic Acids Res*. 2018. **46**: W396–W401.

35 **Garcia, K. C., Tallquist, M. D., Pease, L. R., Brunmark, A., Scott, C. A., Degano, M., Stura, E. A. et al.**, T cell receptor interactions with syngeneic and allogeneic ligands: Affinity measurements and crystallization. *Proc. Natl. Acad. Sci.* 1997. **94**: 13838–13843.

36 **Kuhns, M. S. and Davis, M. M.**, Disruption of extracellular interactions impairs T cell receptor-CD3 complex stability and signaling. *Immunity* 2007. **26**: 357–369.

37 **Robbins, P. F., Li, Y. F., El-Gamil, M., Zhao, Y., Wargo, J. A., Zheng, Z., Xu, H. et al.**, Single and dual amino acid substitutions in TCR CDRs can enhance antigen-specific T cell functions. *J. Immunol.* 2008. **180**: 6116–6131.

38 **Sharma, P. and Kranz, D. M.**, Subtle changes at the variable domain interface of the T-cell receptor can strongly increase affinity. *J. Biol. Chem.* **2017**. https://doi.org/10.1074/jbc.M117.814152.

39 **Malecek, K., Zhong, S., McGary, K., Yu, C., Huang, K., Johnson, L. A., Rosenberg, S. A. et al.**, Engineering improved T cell receptors using an alanine-scan guided T cell display selection system. *J. Immunol. Methods.* 2013. **392**: 1–11.

40 **Ohta, R., Demachi-Okamura, A., Akatsuka, Y., Fujiwara, H. and Kuzushima, K.**, Improving TCR affinity on 293T cells. *J. Immunol. Methods* 2019. **466**: 1–8.

41 **Liu, X., Jiang, S., Fang, C., Yang, S., Olalere, D., Pequignot, E. C., Cogdill, A. P. et al.**, Affinity-tuned ErbB2 or EGFR chimeric antigen receptor T cells exhibit an increased therapeutic index against tumors in mice. *Cancer Res*. 2015. **75**: 3596–3607.

42 **Kerkar, S. P., Sanchez-Perez, L., Yang, S., Borman, Z. A., Muranski, P., Ji, Y., Chinnasamy, D. et al.**, Genetic engineering of murine CD8+ and CD4+ T cells for preclinical adoptive immunotherapy studies. *J. Immunother.* 2011. **34**: 343–352.

43 **Van Den Ent, F. and Löwe, J.**, RF cloning: a restriction-free method for inserting target genes into plasmids. *J. Biochem. Biophys. Methods.* 2006. **67**: 67–74.

44 **Akatsuka, Y., Goldberg, T. A., Kondo, E., Martin, E. G., Obata, Y., Morishima, Y., Takahashi, T. et al.**, Efficient cloning and expression of HLAclass I cDNA in human B-lymphoblastoidcell lines. *Tissue Antigens*. 2002. **59**: 502–511.

45 **Pascolo, S., Bervas, N., Ure, J. M., Smith, A. G., Lemonnier, F. A. and Pérarnau, B.**, HLA-A2.1–restricted education and cytolytic activity of CD8+ T lymphocytes from β2 microglobulin (β2m) HLA-A2.1 monochain transgenic H-2Db β2m double knockout mice. *J. Exp. Med.* 1997. **185**: 2043–2051.

46 **Cossarizza, A., Chang, H., Radbruch, A., Acs, A., Adam, D., Adam-Klages, S., Agace, W. W. et al.**, Guidelines for the use of flow cytometry and cell sorting in immunological studies (second edition). *Eur. J. Immunol.* 2019. **49**: 1457–1973.

Abbreviations: **ACT**: adoptive T-cell therapy · **AID**: activation-induced cytidine deaminase · **CAR**: chimeric antigen receptor · **CD**: cluster of differentiation · **CPRG**: chlorophenolred-ß-D-galactopyranoside · **CTA**: cancer testis antigen · **CTL**: cytotoxic T cell · **EC_{50}**: Effective Concentration 50% · **pMHC**: peptide-MHC · **SHM**: somatic hypermutation · **TAA**: tumor-associated antigen · **TetR**: tetracycline repressor

Full correspondence: Prof. Lea Eisenbach, Department of Immunology, Weizmann Institute of Science, Rehovot 76100, Israel
e-mail: lea.eisenbach@weizmann.ac.il

Received: 7/10/2020
Revised: 7/12/2020
Accepted: 1/4/2021
Accepted article online: 23/3/2021